Scanning tunneling spectroscopy investigations of superconducting-doped topological insulators: Experimental pitfalls and results

Stefan Wilfert, Paolo Sessi, Zhiwei Wang, Henrik Schmidt, M. Carmen Martínez-Velarte, Seng Huat Lee, Yew San Hor, Alexander F. Otte, Yoichi Ando, Weida Wu, and Matthias Bode

Scanning tunneling spectroscopy investigations
of superconducting–doped topological insulators:
Experimental pitfalls and results

Stefan Wilfert,[1, *] Paolo Sessi,[1] Zhiwei Wang,[2] Henrik Schmidt,[1]

M. Carmen Martínez-Velarte,[3] Seng Huat Lee,[4, †] Yew San Hor,[4]

Alexander F. Otte,[3] Yoichi Ando,[2] Weida Wu,[1, 5] and Matthias Bode[1, 6]

[1] *Physikalisches Institut, Experimentelle Physik II,*

Universität Würzburg, Am Hubland, 97074 Würzburg, Germany

[2] *Physics Institute II, University of Cologne, 50937 Cologne, Germany*

[3] *Department of Quantum Nanoscience,*

Kavli Institute of Nanoscience, Delft University of Technology,

Lorentzweg 1, 2628 CJ Delft, The Netherlands

[4] *Department of Physics, Missouri University of*

Science and Technology, Rolla, MO 65409, USA

[5] *Department of Physics and Astronomy,*

Rutgers University, Piscataway, New Jersey, 08854, USA

[6] *Wilhelm Conrad Röntgen-Center for Complex Material Systems (RCCM),*

Universität Würzburg, Am Hubland, 97074 Würzburg, Germany

(Dated: August 2, 2018)

Abstract

Recently the doping of topological insulators has attracted significant interest as a potential route towards topological superconductivity. Because many experimental techniques lack sufficient surface sensitivity, however, a definite proof of the coexistence of topological surface states and surface superconductivity is still outstanding. Here we report on highly surface sensitive scanning tunneling microscopy (STM) and spectroscopy (STS) experiments performed on Tl-doped Bi_2Te_3, a three-dimensional topological insulator which becomes superconducting in the bulk at $T_C = 2.3\,\mathrm{K}$. Landau level spectroscopy as well as quasiparticle interference mapping clearly demonstrated the presence of a topological surface state with a Dirac point energy $E_D = -(118 \pm 1)\,\mathrm{meV}$ and a Dirac velocity $v_D = (4.7 \pm 0.1) \cdot 10^5\,\mathrm{m/s}$. Tunneling spectra often show a superconducting gap, but temperature- and field-dependent measurements show that both T_C and $\mu_0 H_C$ strongly deviate from the corresponding bulk values. Furthermore, in spite of a critical field value which clearly points to type-II superconductivity, no Abrikosov lattice could be observed. Experiments performed on normal-metallic Ag(111) prove that the gapped spectrum is only caused by superconducting tips, probably caused by a gentle crash with the sample surface during approach. Nearly identical results were found for the intrinsically n-type compound Nb-doped Bi_2Se_3. Our results suggest that the superconductivity in superconducting-doped V-VI topological insulators does not extend to the surface where the topological surface state is located.

I. INTRODUCTION

It has quite early been theoretically recognized that the lack of spin- and spatial-rotation symmetries in p-wave superconductors leads to unconventional textures of the order parameter which may result in domain walls and quasiparticle excitations with vanishing excitation energies, so-called zero modes.[1,2] Whereas early theories were originally designed to describe superconductors in symmetries characteristic for the fractional quantum Hall effect (FQHE), the discovery of three-dimensional topological insulators (TIs),[3] which at the same time possess a gapped bulk state and a gapless surface state, opened additional avenues towards a realization of these collective quantum phenomena and their potential application in quantum computation.[4] In this context zero energy Majorana bound states (MBS), which represent the most simple non-Abelian excitation of Moore-Read states,[5] are particularly auspicious as they would allow the non-local storage of quantum bits, thereby promising a larger robustness against local sources of decoherence.[6,7]

Various routes towards the realization of topological superconductors have been pursued. For example, it has been theoretically proposed that the proximity of an ordinary s-wave superconductor with a strong TI results in $p_x + ip_y$ superconductivity which can support MBS in vortices.[8] Indeed, planar heterostructure could successfully be prepared by the epitaxial growth of topological insulators epitaxially grown on superconducting $NbSe_2$.[9,10] In agreement with theoretical expectations an in-gap zero-bias conductance peak was found in magnetic vortices in proximity-coupled Bi_2Te_3 films.[11]

Another route may be the self-organized growth or atom-by-atom assembly of one-dimensional magnetic chains on strongly spin-orbit–coupled superconductors. Model calculations indicated that single-atomic chains with a modulated (helical) spin structure exhibit a non-trivial topological ground state with MBS at the two chain termination points.[12] Although a zero-bias conductance peak was indeed observed in scanning tunneling spectroscopy (STS) experiments performed on self-organized Fe chains on Pb(110),[13] the interpretation of these results remains controversial.[14]

Especially from a materials perspective the intercalation or doping of bismuth chalcogenides (Bi_2Se_3 or Bi_2Te_3) represents another promising and frequently pursued approach towards the realization of topological superconductors. Throughout the remainder of this contribution, the term "intercalation" will refer to the inclusion of atoms into a van der

Waals gap between two layers of the host material, whereas the term "doping" refers to impurities in regular lattice sites. Table I summarizes experimental key results of materials combinations relevant in the context of our work. The left column of Tab. I lists the chemical formula together with the nominal concentration of the doping element. The following three columns, from left to right, recapitulate the employed experimental techniques, the reported critical temperature T_C and the critical field $\mu_0 H_C$, respectively. The second column from the right indicates whether the existence of the topological surface state (TSS) has explic-

TABLE I. Overview of experimental studies analyzing potential superconducting-doped topological insulators. The critical field $\mu_0 H_C$ was obtained for applied fields perpendicular to the sample surface.

Material (concentration)	Experimental techniques	T_C	$\mu_0 H_C$	TSS verified?	Ref.
$Cu_x Bi_2 Se_3$					
($0.10 \leq x \leq 0.15$)	transport, XRD, TEM, STM	3.8 K	1.7 T	No	[15]
($x = 0.25$)	transport, magnetometry	3.3 K	not shown	Yes	[16]
($x = 0.3$)	point-contact spectroscopy	3.2 K	not shown	No	[17]
($x = 0.2$)	STM, STS	not shown	1.7 T (at 0.95 K)	No	[18]
($x = 0.3$)	NMR	3.4 K	not shown	No	[19]
($x = 0.3$)	specific heat	3.2 K	not shown	No	[20]
$Sr_x Bi_2 Se_3$					
($x \leq 0.065$)	transport	2.57 K	≈ 1 T	Yes	[21]
($x = 0.1$)	transport, SEM, TEM	2.9 K	1.4 T (at 0 K)	No	[22]
($x = 0.2$)	STM, STS	5 K	≥ 5 T	Yes	[23]
$Tl_x Bi_2 Te_3$					
($x = 0.6$)	transport	2.28 K	1.06 T	No	[24]
($x = 0.5$)	ARPES	not shown	not shown	Yes	[25]
$Nb_x Bi_2 Se_3$					
($x = 0.25$)	transport, STM, ARPES	3.6 K	0.15 T (at 2 K)	Yes	[26]
($x = 0.25$)	torque magnetometry	3 K	0.6 T	No	[27]

itly been proven experimentally. We would like to emphasize that all measurements were either carried out at the Fermi level or it was shown that the TSS crosses E_{F}, a crucial condition towards topological superconductivity. Finally, the column at the very right cites the reference.

$Cu_x Bi_2 Se_3$ with $0.10 \leq x \leq 0.15$ was the first intercalated topological material for which a superconducting transition with a transition temperature of $3.8\,\mathrm{K}$ was claimed.[15] X-ray diffraction (XRD) experiments in combination with transmission electron microscopy (TEM) confirmed that Cu was intercalated into the van der Waals gap of $Bi_2 Se_3$ with "long or short range order".[15] Torque magnetometry measurements that showed pronounced quantum oscillations in high magnetic field were interpreted as evidence for topological properties, although at a slightly different doping level ($x = 0.25$).[16] Furthermore, the observation of a zero-bias conduction peak in point-contact spectroscopy experiments which vanishes above $1.15\,\mathrm{K}$ and $0.8\,\mathrm{T}$ indicated the existence of Majorana fermions.[17]

An STM/STS study performed on $Cu_x Bi_2 Se_3$ with $x = 0.2$ revealed an inhomogeneous sample that only exhibits superconductivity in some surface regions.[18] Also other studies reported a rather low superconducting volume fraction which could be improved by avoiding substitutional Cu defects.[28] In the superconducting regions of cleaved $Cu_{0.2}Bi_2 Se_3$ the STM/STS study of Levy *et al.*[18] mostly showed a gap without any zero-bias anomaly which could well be fitted by BCS theory, suggesting classical *s*-wave superconductivity. Interestingly, some results occasionally obtained at particularly low tunneling resistance (close tip–sample distance) exhibited a zero-bias peak. Similar to what we will discuss below, this observation was ascribed to a tip which "became contaminated and possibly superconducting after crashing into the sample".[18] However, the study of Levy *et al.*[18] does not discuss whether the superconducting regions also support the topological surface state. Contradictory to the pairing mechanism suggested by these STS data, nuclear magnetic resonance (NMR)[19] and specific heat[20] measurements demonstrated a broken spin-rotation symmetry indicating a pseudo spin-triplet state in $Cu_x Bi_2 Se_3$.

Sr-intercalated and Sr-doped $Bi_2 Se_3$ was investigated by resistivity experiments. Whereas no superconductivity was found for the doped sample, a superconducting transition temperature of $2.57\,\mathrm{K}$ was reported for Sr-intercalated $Bi_2 Se_3$. Magnetic field-dependent measurements revealed a critical field of roughly $1\,\mathrm{T}$ and quantum oscillations verifying the presence of a surface state.[21] In another transport study the influence of the nominal Sr

content x was analyzed and $x = 0.1$ was declared as the optimal level leading to a critical temperature of $2.9\,\mathrm{K}$ and a critical field of $1.4\,\mathrm{T}$ if interpolated to zero temperature.[22] In combined STM/STS measurements on $\mathrm{Sr_{0.2}Bi_2Se_3}$ two kinds of surface areas were found.[23] Whereas the clean surface with large atomically smooth terraces showed no signs of superconductivity, sample areas decorated with clusters of varying size revealed a V-shaped gap. Based on Landau level spectroscopy it was claimed that a proper topological surface state is present, even though the very narrow energy range over which the Landau levels could be observed severely complicates the determination if the Landau level dispersion relation indeed follows a Dirac-like behavior.[23] Furthermore, the values reported in Ref. 23 for the critical temperature ($T_\mathrm{C} = 5\,\mathrm{K}$) and the critical field ($\mu_0 H_\mathrm{C} \geq 5\,\mathrm{T}$) by far exceed what was found in above-mentioned studies.[21,22]

Recently, superconductivity with a critical temperature of $2.28\,\mathrm{K}$ and critical field of $1.06\,\mathrm{T}$ was found in $\mathrm{Tl}_x\mathrm{Bi_2Te_3}$ at optimal Tl content $x = 0.6$.[24] X-ray diffraction showed sharp reflections similar to pristine $\mathrm{Bi_2Te_3}$ indicating a good crystalline quality. An angle-resolved photoemission spectroscopy (ARPES) study of $\mathrm{Tl}_x\mathrm{Bi_2Te_3}$ with a slightly lower Tl content ($x = 0.5$) showed that the Dirac surface state is well isolated from bulk bands making this sample ideal to study topological superconductivity.[25]

Also Nb intercalation of $\mathrm{Bi_2Se_3}$ leads to superconductivity with a critical temperature of $3.6\,\mathrm{K}$ and a critical field of $0.15\,\mathrm{T}$ at $2\,\mathrm{K}$. ARPES clearly demonstrated the existence of a Dirac-like surface state with a Dirac point energy lying roughly $300\,\mathrm{mV}$ below the Fermi level.[26] Torque magnetometry showed a strong coupling between superconductivity and the crystal symmetry leading to bulk nematic order in the superconducting ground state[27] similar to the findings in $\mathrm{Cu}_x\mathrm{Bi_2Se_3}$.[19,20]

Although a large number of reports discusses the potential existence of topological superconductivity in doped or intercalated topological host materials,[15–18,21–27] we have to conclude that none of these references at the same time convincingly proves the *coexistence* of surface superconductivity and a topological surface state with a Dirac-like dispersion. Most transport studies[15,17,21,22,24,26,27] are essentially bulk sensitive, i.e., even a large volume fraction cannot safely assure that superconductivity extends all the way up to the terminating quintuple layer which supports the topological surface state. Others show indisputable evidence for surface superconductivity but fail to show the existence of the topological surface state (TSS).[18] Only one study claims the observation of surface superconductivity and

the TSS.[21] However, even though the very high critical field of $5\,\mathrm{T}$ suggests a type-II superconductor no Abrokosov lattice is shown,[21] thereby questioning the validity of these results.

Here we report on our attempts to verify the coexistence of topological surface states and surface superconductivity on cleaved surfaces of $\mathrm{Tl_{0.6}Bi_2Te_3}$ and $\mathrm{Nb_{0.25}Bi_2Se_3}$. Especially Tl-doped $\mathrm{Bi_2Te_3}$ is unique as—contrary to other materials—it is p-doped. In heavily n-doped materials the Fermi level is well inside the conduction band such that bulk and surface superconductivity may easily be confused. In contrast, we can disentangle topological states from bulk electronic properties for p-type Tl-doped $\mathrm{Bi_2Te_3}$. Landau level spectroscopy in combination with quasiparticle interference mapping on one hand clearly demonstrates the presence of a topological surface state in both compounds. On the other hand, in neither case we were able to find clear evidence for surface superconductivity down to the lowest possible measurement temperature of $300\,\mathrm{mK}$. Even though superconducting gaps were regularly observed in STS data at high energy resolution, several inconsistencies indicate that these results are most likely caused by an unintentional coating of the tip apex with superconducting material, possibly in form of a small cluster. This interpretation is supported by values for the critical temperature and the critical field which deviated strongly from corresponding values measured with bulk sensitive methods.

II.   EXPERIMENTAL PROCEDURES

The growth of Tl-doped $\mathrm{Bi_2Te_3}$ was performed by mixing high-purity elemental shots of Tl (99.99%), Bi (99.9999%), and Te (99.9999%) that were cleaned in order to remove oxide layers. The mixture was sealed in an evacuated quartz tube and heated to $1123\,\mathrm{K}$ for $48\,\mathrm{h}$. The tube was cooled to $823\,\mathrm{K}$ with a rate of $5\,\mathrm{K/h}$, followed by a quench in ice-water [see Refs. 24 and 29 for further details]. Due to the high room temperature mobility of Tl atoms in $\mathrm{Tl_xBi_2Te_3}$ and the associated reduction of the superconducting volume fraction,[24] samples were stored at liquid nitrogen temperatures or below.

Scanning tunneling microscopy (STM) and spectroscopy (STS) experiments were carried out with two scanning tunneling microscopes, each covering a dedicated temperature range. Measurements with a minimal temperature $T_{\min} = 1.5\,\mathrm{K}$ were performed with a home-built cryogenic scanning tunneling microscope which is equipped with a superconducting magnet that supplies a magnetic field of up to $12.5\,\mathrm{T}$ perpendicular to the sample surface.

Experiments at lower temperature ($T = 300 \, \mathrm{mK}$) were executed with a commercial Unisoku USM-1300. For all measurements we used electro-chemically etched W tips. Topographic images were recorded in the constant-current mode. The bias voltage is applied to the sample, i.e., negative (positive) voltages correspond to occupied (unoccupied) sample states, respectively. Spectroscopy data were obtained under open feedback loop conditions by adding a small modulation voltage U_{mod} to the bias voltage U by means of a lock-in amplifier.

The samples were glued on a sample holder, introduced into the ultra-high vacuum system via a load lock, and cleaved at room temperature at a pressure $p \leq 5 \cdot 10^{-10} \, \mathrm{mbar}$. Immediately after cleavage the pristine sample was inserted into the STM. During tip conditioning, which was performed by dipping the tip apex into a clean Ag(111) surface, the sample was stored in a garage inside the LHe shield at temperatures close to $4.2 \, \mathrm{K}$.

III.   RESULTS AND DISCUSSION

A.   Tl-doped Bi_2Te_3

1.   The topological surface state

Figure 1(a) shows the topography of a cleaved $Tl_{0.6}Bi_2Te_3$ sample. The inset presents a zoomed-in STM image with atomic resolution. The measured lattice constant of $(4.4 \pm 0.2) \, \mathrm{\AA}$ is in good agreement with the bulk lattice constant of $4.38 \, \mathrm{\AA}$. In a $50 \times 50 \, \mathrm{nm}^2$ scan area we find a total of (220 ± 15) defects, i.e., far below the number of 9,000 Tl atoms expected within the first quintuple layer of $Tl_{0.6}Bi_2Te_3$. In fact, by analyzing the appearance of defects in STM images we find that the vast majority of them closely resemble defects which are also characteristic for pristine p-doped Bi_2Te_3, i.e., antisites of Bi in the top and the bottom Te plane of the first quintuple layer.[30] Based on these data one would naively expect that Tl does not occupy sites within Bi_2Te_3 quintuple layers but is rather located in van der Waals gaps between quintuple layers. This interpretation is, however, inconsistent with earlier neutron scattering and X-ray diffraction studies where an intercalated site could be excluded.[24] Instead, these data indicated that the Tl atoms primarily occupy Bi sites, whereas the kicked-out Bi atoms in turn result in Bi_{Te} antisites, such that the system as a whole remains in the tetradymite structure. Effectively, the chemical formula of $Tl_{0.6}Bi_2Te_3$ approximately becomes $(Tl_{0.27}Bi_{0.73})_2(Bi_{0.11}Tl_{0.89})_3$. We can only speculate why Bi antisites,
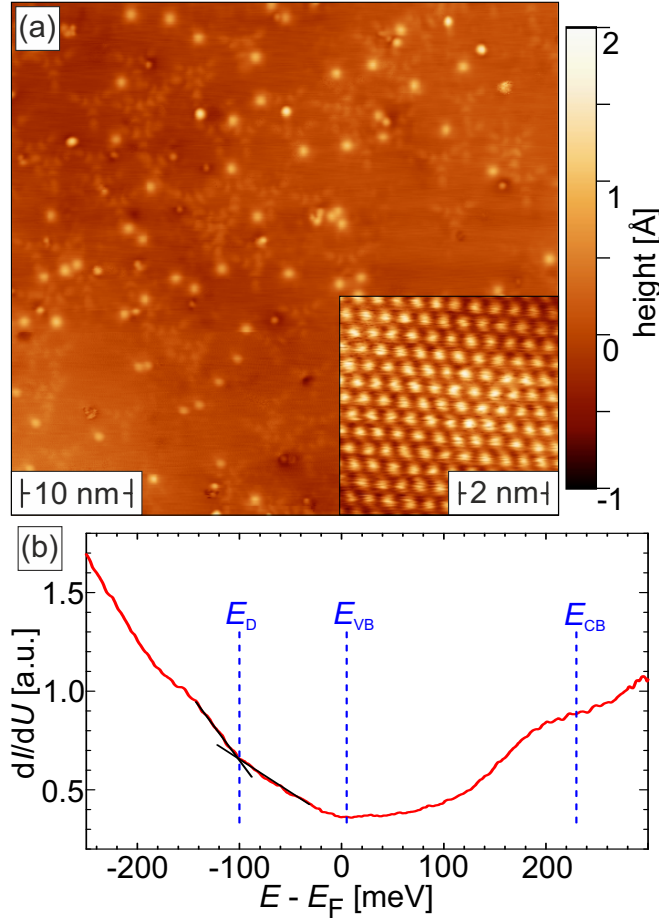
FIG. 1. (a) Topographic image of cleaved $Tl_{0.6}Bi_2Te_3$. Defects characteristic for p-doped Bi_2Te_3 can be recognized. No signs of Tl intercalation are visible. The inset shows an atomic resolution image. (b) Differential conductance (dI/dU) spectrum of $Tl_{0.6}Bi_2Te_3$ recorded on the clean surface at a lateral distance of more than 3 nm from a defect. Dirac point energy (E_D), valence band maximum (E_{VB}), and conduction band minimum (E_{CB}) are marked with blue dashed lines. Scan/stabilization parameters: $T = 1.7$ K; (a) $U = -0.3$ V, $I = 50$ pA, (inset) $U = -0.2$ V, $I = 50$ pA; (b) $U_{set} = -0.4$ V, $I_{set} = 100$ pA, $U_{mod} = 5$ mV.

which are well visible on cleaved Bi_2Te_3,[30] might have remained undetected in our STM experiments on $Tl_{0.6}Bi_2Te_3$. Potentially, the bias voltage and, therefore, the energy window chosen here was unsuitable for detecting these antisites in topography.

Figure 1(b) presents an overview scanning tunneling spectrum of $Tl_{0.6}Bi_2Te_3$. Similar to the results presented in Ref. 31, the Landau level spectroscopy data which will be described below can consistently be explained if we assume that the top of the bulk valence band is energetically located at the minimum differential conductance dI/dU. Correspondingly, the flat part of the shoulder in the unoccupied energy range marks the bottom of the conduction band at $E_{CB} = (230 \pm 10)$ meV. Similar to pristine Bi_2Te_3, the Dirac point lies inside the valence band and can be recognized by a change of slope in the dI/dU signal. As indicated by black lines in Fig. 1(b) this linear approximation procedure results in a Dirac energy $E_D = (-100 \pm 20)$ mV.

Whereas the procedures performed to analyze the data of Fig. 1(b) result in a relatively
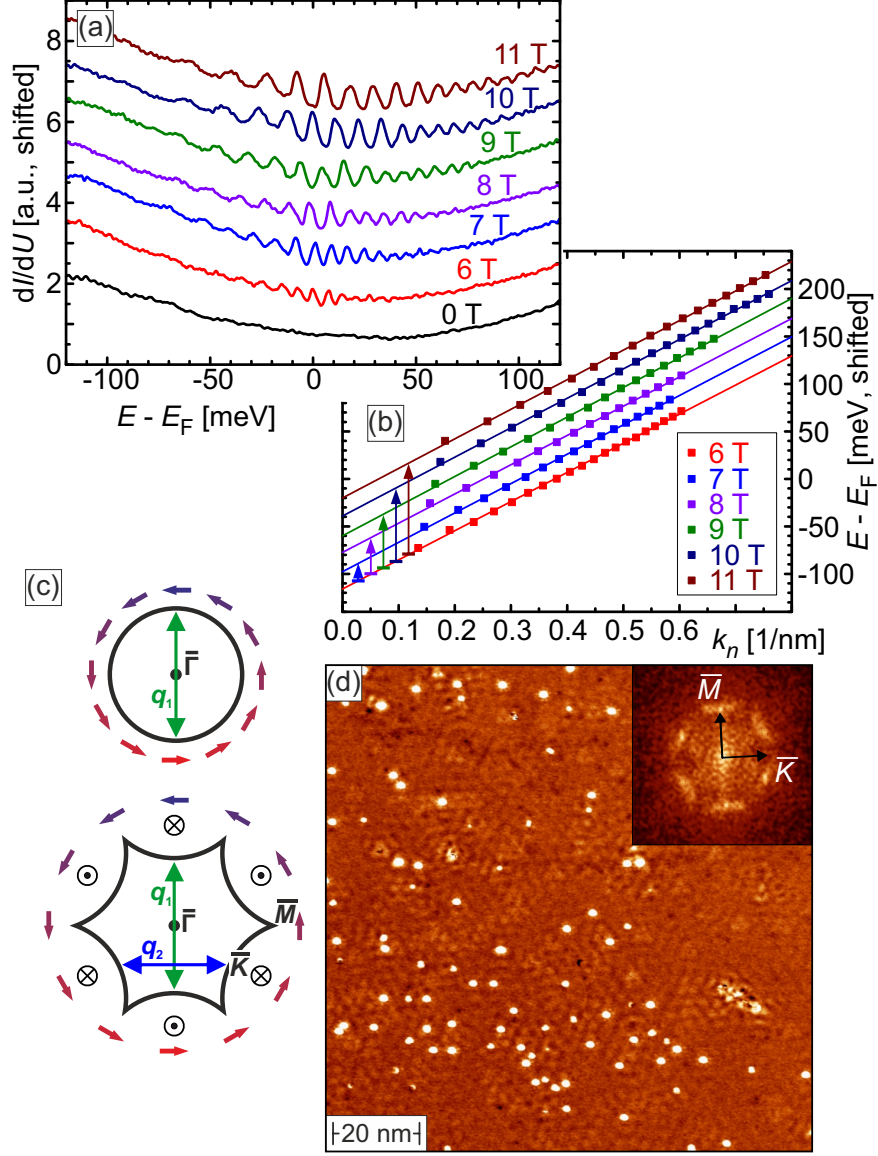
FIG. 2. (a) STS data of $Tl_{0.6}Bi_2Te_3$ measured at various magnetic fields at $T = 1.7$ K. (b) Landau level energies plotted versus k_n confirming the linear dependence expected for a TSS. (c) Schematic equipotential surface (black), in-plane spin polarization (blue/red arrows), and potential scattering vectors (q_1/q_2) for a TI close to the Dirac point (upper panel) and in the warped energy regime (lower). (d) QPI map of $Tl_{0.6}Bi_2Te_3$ and its Fourier transformation in the inset ($T = 4.8$ K). No backscattering can be recognized. Scan parameters: (a) $U = -150$ mV, $I = 600$ pA, $U_{\mathrm{mod}} = 1$ mV; (d) $U = 400$ mV, $I = 50$ pA, $U_{\mathrm{mod}} = 10$ mV.

large error bar, Landau level spectroscopy (LLS) permits a much more accurate determination of the dispersion relation of Dirac-like quasiparticles. Fig. 2(a) shows STS data of

$Tl_{0.6}Bi_2Te_3$ measured at zero field (black) and at various externally applied magnetic fields up to 11 T. The zero-field spectrum is similar to the one presented in Fig. 1(b). At high magnetic fields a sequence of peaks appear in the energy range of ± 100 meV. When increasing the magnetic field strength the individual peaks become more intense and their energy separation increases, such that more peaks become visible in a wider and wider energy range.

These peaks indicate the evolution of a series of Landau levels (LL). In Dirac materials the LL energies are given by the equation

$$E_n = E_D + \text{sgn}(n)v_D \cdot \sqrt{2\hbar e|n|B} = E_D + \text{sgn}(n)v_D\hbar k_n, \tag{1}$$

where E_D is the Dirac energy, v_D the Dirac velocity, n the LL index, and B the magnetic field perpendicular to the sample surface. In the case of $Tl_{0.6}Bi_2Te_3$ all peaks visible in Fig. 2(a) correspond to electron-like Landau levels; hole-like Landau levels could not be detected, in agreement with earlier experiments on pristine Bi_2Te_3.[32] For further analysis we performed a background subtraction for the data presented in Fig. 2(a) and fitted the Landau level peaks by Gaussian functions. The obtained Landau level energies are plotted versus k_n in Fig. 2(b). The results nicely match the expected linear dependence, thereby confirming the existence of a Dirac like surface state. Fitting the experimental data with Eq. (1) results in a Dirac point energy $E_D = -(118 \pm 1)$ meV and a Dirac velocity $v_D = (4.7 \pm 0.1) \cdot 10^5$ m/s.

Another characteristic property of topological surface states is the absence of backscattering. It has been shown that quasiparticle interference mapping can visualize the scattering behavior of topological surface states.[33–35] Fig. 2(c) illustrates potential scattering vectors between nested parts of the equipotential surface of a TI in close proximity to the Dirac energy (upper panel) and further away from the Dirac point (lower panel), where the symmetry of the crystal lattice leads to warping with a significant out-of-plane spin polarization caused by spin-orbit coupling.[36] Close to the Dirac energy the only nested (parallel) parts of the almost circular equipotential surface are located at opposite k values, i.e., states which also possess an opposite spin polarization. Consequently, backscattering [see scattering vector q_1 in Fig. 2(c)] is forbidden as long as time-reversal symmetry is maintained. With increasing energy separation from the Dirac point spin-orbit effects which become more relevant, eventually deform the the equipotential surface to a snowflake-like shape. This opens further scattering channels (q_2) which are allowed due to the resulting out-of-plane component to the spin polarization and expected to occur in the $\overline{\Gamma M}$ direction of the sur-

face Brillouin zone.[36] Indeed, Fourier transformation of the quasiparticle interference map shown in Fig. 2(d) which was measured at a bias voltage $U = 400\,\text{mV}$, i.e., at an energy about $0.5\,\text{eV}$ above the Dirac point, shows intensity maxima along this direction, whereas no intensity is found along the backscattering direction $\overline{\Gamma K}$ (see inset).

2. Superconducting properties

The results presented so far confirm that the surface of Tl-doped Bi_2Te_3 exhibits a topological surface state with a Dirac point about $100\,\text{meV}$ below the Fermi level and a valence band maximum just above the Fermi level. These values slightly deviate from what has been observed by Trang et al. [25] for as-grown (fresh) $Tl_{0.6}Bi_2Te_3$ by ARPES ($E_D = -60\,\text{meV}$). In the same study[25] it was shown that sample storage at a pressure $p = 2 \times 10^{-10}\,\text{torr}$ for $12\,\text{h}$ results in surface aging-induced n-type shift of the surface chemical potential by about $220\,\text{meV}$, i.e., far into the conduction band. Even though the shift of $58\,\text{mV}$ observed here is much smaller, some surface band bending is undeniably observed in our STS data, the origin of which remains to be investigated. We would like to emphasize, however, that the very low surface density of states at the Fermi level is rather favorable for the unanimous identification of superconducting properties of Dirac electrons, as long as the surface band bending does not prevent to induce superconductivity from the bulk into the surface Dirac electrons via a proximity effect.

To investigate potential superconducting properties of cleaved $Tl_{0.6}Bi_2Te_3$ we performed high resolution spectroscopy experiments close to the Fermi energy. An experimental result obtained at a nominal temperature $T \approx 1.5\,\text{K}$ is presented as a black line in Fig. 3(a). A U-shaped superconducting gap with an almost vanishing zero-bias $\text{d}I/\text{d}U$ signal and pronounced coherence peaks at $E \approx 1.3\,\text{meV}$ is clearly visible. As shown in Fig. 3(b), the gap size decreases with increasing temperature until it vanishes roughly at $5.0\,\text{K}$, a value which is more than twice the reported critical temperature of bulk $Tl_{0.6}Bi_2Te_3$, $T_C^{\text{bulk}} = 2.3\,\text{K}$.[24] A similar discrepancy is found in the field-dependent STS data displayed in Fig. 3(c). In qualitative agreement with the expected behavior the gap size decreases with increasing magnetic field. However, even at $4.5\,\text{T}$ a tiny gap can still be recognized. Similar to the temperature dependence the critical magnetic field, if it was extracted from the experimental data presented in Fig. 3(c), would substantially exceed the respective value of bulk $Tl_{0.6}Bi_2Te_3$,

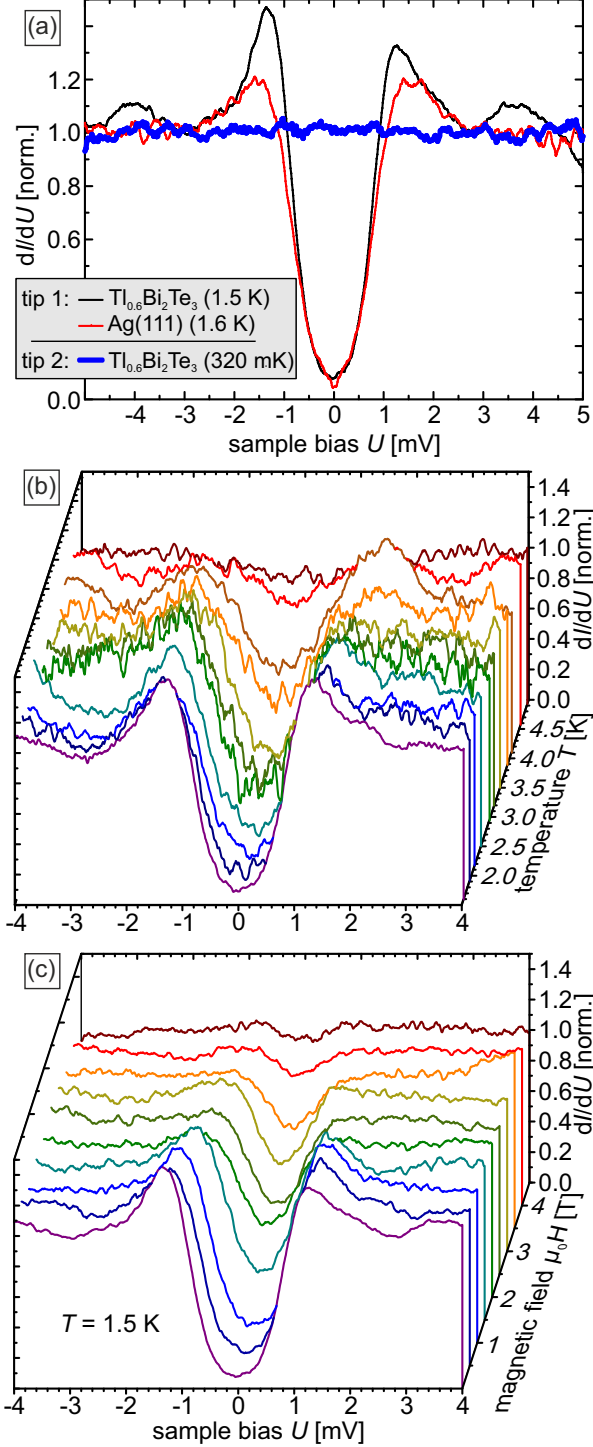FIG. 3. (a) Normalized dI/dU spectra of $Tl_{0.6}Bi_2Te_3$. The spectrum taken with tip 1 shows a superconducting gap at $T = 1.5\,\mathrm{K}$ (black line). However, the same tip exhibits a very similar gap on Ag(111) (red), indicating that a superconducting cluster was accidentally picked up, presumably due to a gentle collision with the sample surface. After careful tip handling even at $T = 0.32\,\mathrm{K}$ no gap can be found (tip 2; blue). (b) Temperature-dependent dI/dU spectra as measured with a superconducting tip. The gap vanishes at 5 K, i.e., a temperature significantly higher than T_C. (c) Field-dependent STS data measured with the very same tip at $T = 1.5\,\mathrm{K}$. The superconducting gap can be recognized up to 4.5 T. Parameters: $U = -5\,\mathrm{mV}$, $I = 50...200\,\mathrm{pA}$, $U_{\mathrm{mod}} = 0.1\,\mathrm{mV}$.

which only amounts to $\mu_0 H_C^{\mathrm{bulk}} \approx 400\,\mathrm{mT}$ at our measurement temperature of 1.5 K.[24]

We would like to emphasize that the observation of a superconducting gap in STS experiments on cleaved $Tl_{0.6}Bi_2Te_3$ was not at all an exception but was instead rather frequent, even if a freshly prepared W tip was used for the experiment. Furthermore, temperature- and field-dependent measurements reliably reproduced the data presented in Fig. 3(b) and

(c). Since the high magnetic field necessary to close the superconducting gap in Fig. 3(c) suggests a type-II superconductor, we expected an inhomogeneous phase where a sufficiently strong applied magnetic field ($H_{\mathrm{app}} > H_{\mathrm{C_1}}$) would lead to magnetic flux quanta penetrating the superconductor, potentially in form of an Abrikosov lattice. Although we have recently successfully observed Abrikosov lattices on Nb(110) (not shown) and the heavy-electron superconductor $TlNi_2Se_2$,[37] we never found any magnetic vortices on cleaved $Tl_{0.6}Bi_2Te_3$.

In order to characterize the probe tip more carefully, we performed STS experiments on a normal-metallic Ag(111) surface. The red curve in Fig. 3(a) shows a high resolution spectrum recorded at $T = 1.6\,\mathrm{K}$ with a tip previously used for scanning a $Tl_{0.6}Bi_2Te_3$ sample. One can recognize a superconducting gap with a very similar shape as for $Tl_{0.6}Bi_2Te_3$ (cf. black spectrum). The small deviations are possibly caused by a slightly higher measurement temperature and the metallic nature of silver which leads to a much higher density of states at the Fermi level. These findings clearly show that the superconducting gap observed in the black curve of Fig. 3 is not caused by the sample itself but by the tip which most likely picked up a superconducting cluster from the $Tl_{0.6}Bi_2Te_3$ sample.

Comparison of our results with a recent temperature- and field-dependent STS study[23] of the potential topological superconductor $Sr_{0.2}Bi_2Se_3$ reveals some surprising similarities. For example, for $Sr_{0.2}Bi_2Se_3$ a critical temperature $T_{\mathrm{C}} \approx 5\,\mathrm{K}$ and a second critical field $\mu_0 H_{\mathrm{C_2}} \approx 5\,\mathrm{T}$ were reported.[23] These values do not only significantly exceed the corresponding bulk values determined by transport,[21,22] they are also strikingly close to what we observe with superconducting tips in Fig. 3. Even though the existence of a second critical field would necessarily imply the formation of magnetic vortices at $H_{\mathrm{C_1}} < H < H_{\mathrm{C_2}}$, their existence has neither been discussed nor experimentally shown in Ref. 23.

Only if we took extreme care to safely approach the tip to the $Tl_{0.6}Bi_2Te_3$ surface by using a very low set point current $I_{\mathrm{set}} \leq 30\,\mathrm{pA}$ and feedback circuit settings which exclude self-resonance we could avoid any tip–sample contact. With these clean W tips we performed measurements on several samples that were previously analyzed by transport measurements. Even though all samples showed bulk superconductivity with transition temperatures close to $2.3\,\mathrm{K}$, we were unable to detect any superconducting gap in the low-bias regime around the Fermi level in our STS experiments, as exemplarily shown by the thick blue line in Fig. 3(a). In combination with the previously discussed observations, i.e., the strong evidence for an (accidental) superconducting probe tip and the absence of flux quanta, these
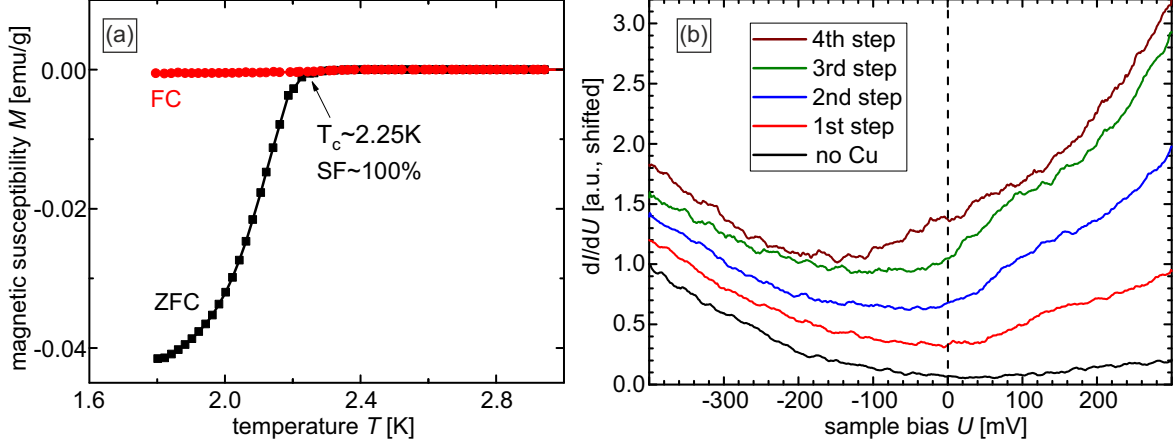
14

FIG. 4. (a) Temperature-dependent magnetic susceptibility measured after STM/STS measurements. No significant changes of critical temperature and the superconducting volume fraction were found. (b) Overview spectroscopy data taken with a W tip on $Tl_{0.6}Bi_2Te_3$ for different Cu doping amounts. With increasing amount of Cu on the sample surface the bulk band gap shifts to lower energies.

measurements exclude that the surface of cleaved $Tl_{0.6}Bi_2Te_3$ is superconducting down to the lowest measurement temperature applied here, i.e., $T = 0.32\,\text{K}$.

This finding might be explained by three scenarios: (i) The sample was superconducting immediately after materials synthesis but later degrades due to aging effects, potentially because of insufficient cooling and the resulting onset of Tl segregation, which could lead to a reduction of the superconducting volume fraction.[24] (ii) Superconductivity only exists in the bulk and the proximity effect on Dirac electrons is too weak to observe any significant Cooper pair formation on the sample surface. (iii) The surface critical temperature of $Tl_{0.6}Bi_2Te_3$ is substantially lower than the corresponding bulk value, $T_C^{\text{bulk}} = 2.3\,\text{K}$.

To check if degradation, scenario (i), is responsible for the absence of surface superconductivity we performed another set of SQUID measurements after STS experiments had been carried out, i.e., the sample initially shipped from the growth lab (University of Cologne) to the STM lab (Universität Würzburg) is, upon completion of STM measurements, shipped back to its origin. Fig. 4(a) shows the resulting temperature-dependent magnetic susceptibility which clearly demonstrates that T_C^{bulk} remains unchanged and that the superconducting volume fraction still amounts close to 100%. Obviously, the small shift of the chemical potential is only present at the surface, whereas the bulk chemical potential remains unchanged

15

throughout the entire experiment.

To test scenario (ii) we increased the density of bulk states around the Fermi energy to potentially boost the coupling between topological Dirac electrons on one hand and the Cooper pairs supported by the $Tl_{0.6}Bi_2Te_3$ bulk on the other hand. This goal was achieved by doping the $Tl_{0.6}Bi_2Te_3$ surface with Cu evaporated onto the cold sample inside the LT-STM, which resulting in well separated Cu adatoms (not shown here). Non-magnetic Cu was chosen to avoid any influences of magnetic moments on the superconductivity. Fig. 4(b) presents overview spectroscopy data measured on pristine $Tl_{0.6}Bi_2Te_3$ and after four consecutive steps of Cu adatoms deposition. With increasing Cu density we observed that the minimum of the dI/dU signal shifts systematically to lower energies. Although we cannot directly detect the top and bottom edge of the valence and conduction band, respectively, it is quite reasonable to assume that the gap shifts accordingly. Obviously, the adatoms donate electrons to $Tl_{0.6}Bi_2Te_3$ and lead to an n-type shift of the chemical potential, a behavior also observed for other $3d$ transition metals on topological insulators.[35] The bulk band gap shifts from the Fermi energy for the pristine sample by about $200\,meV$ towards the occupied states, eventually resulting in a Fermi level that lies well inside the conduction band after four steps of doping. In spite of this significant electron doping, we could not detect any sign of superconductivity in Cu-doped $Tl_{0.6}Bi_2Te_3$ down to $T = 1.5\,K$ (high resolution spectra not shown here).

The surface-related downward band bending effects discussed above possibly results in a surface which is effectively decoupled from the p-doped bulk. This decoupling could lead to scenario (iii), i.e., a surface critical temperature which is substantially lower than the corresponding bulk value. In fact we could not detect any sign of surface superconductivity in our STS measurements down the lowest possible sample temperature in our study which was more than a factor of 6 lower than $T_C^{bulk} = 2.3\,K$. As will be discussed below the issue of a p–n junction which isolates the surface from the bulk might be overcome by p-type doping the $Tl_{0.6}Bi_2Te_3$ surface.

B.   Nb-intecalated Bi_2Se_3

In an attempt to potentially detect superconductivity on an intrinsically n-doped super-conducting topological insulator, we also investigated the intercalation material $Nb_xBi_2Se_3$
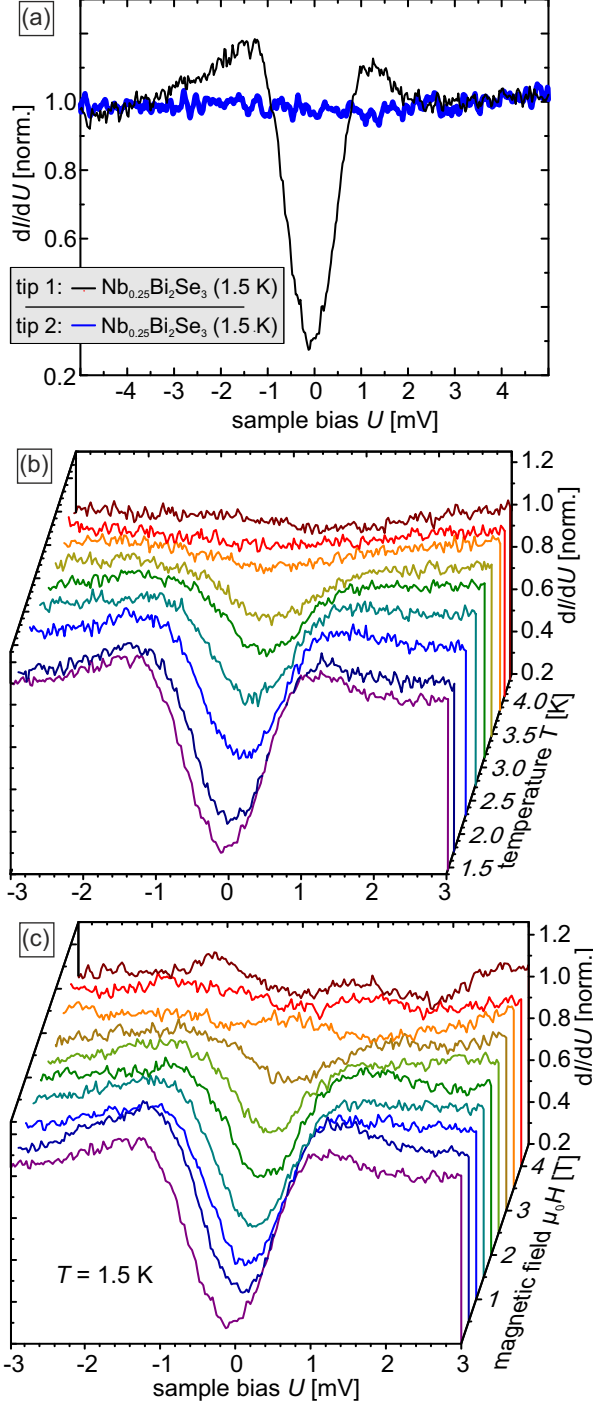
FIG. 5. (a) High resolution STS data on Nb-intercalated Bi_2Se_3 acquired with a superconducting (1; black) and a normal-metallic W tip (2; blue) at a nominal temperature $T = 1.5\,\mathrm{K}$. While for tip 1 a pronounced gap is visible no superconductivity can be recognized with tip 2. (b) Temperature-dependent normalized dI/dU signal taken on $Nb_xBi_2Se_3$ with a superconducting tip. (c) Magnetic field-dependent STS data taken with superconducting tip. The gap can be recognized up to about 3 T. For higher fields additional variations caused by the fine structure of the Landau levels are visible. Stabilization parameters: $U = -5\,\mathrm{mV}$, $I = 200\,\mathrm{pA}$, $U_{\mathrm{mod}} = 0.1\,\mathrm{mV}$.

which exhibits a bulk critical temperature $T_{\mathrm{c}}^{\mathrm{bulk}} = 3.2\,\mathrm{K}$.[26] Similar to what has been shown in Fig. 2(b) for $Tl_{0.6}Bi_2Te_3$ we could also confirm the existence of a topological surface state for $Nb_xBi_2Se_3$ based on the linear dispersion of the LL peaks in a strong external magnetic field, resulting in a Dirac point energy $E_{\mathrm{D}} = -(350 \pm 2)\,\mathrm{meV}$ (not shown here). Regarding superconductivity, Fig. 5(a) shows high resolution STS data obtained with various tips. As already described in the context of Fig. 3 for $Tl_{0.6}Bi_2Te_3$, we also detected superconducting

gaps on $Nb_xBi_2Se_3$ with numerous tips, as shown by the spectrum colored black in Fig. 5(a). Temperature- and magnetic field-dependent dI/dU spectra measured with such a tip are presented in Fig. 5(b) and (c), respectively. These data reveal that both the critical temperature and the critical field are very similar to the values detected with superconducting tips on $Tl_{0.6}Bi_2Te_3$ [cf. Fig. 3(b) and (c)], whereby the critical magnetic field is substantially higher than the bulk value $\mu_0 H_C^{bulk} \approx 200\,mT$ reported for $T = 1.5\,K$.[26] Furthermore, we could not detect any hint of magnetic flux quanta or an Abrikosov lattice. These observations together with the fact that we found no gap with some particularly carefully handled STM tips indicate that also for $Nb_xBi_2Se_3$ the gap does not represent a property of the sample but is rather caused by a superconducting cluster which was unintentionally picked up by the tip.

C. Discussion

Our investigation of the electronic properties of the doped topological insulators $Tl_{0.6}Bi_2Te_3$ and $Nb_xBi_2Se_3$ reveals some striking similarities. Quasiparticle interference and Landau level spectroscopy (LLS) data confirm that the surfaces of both materials exhibit a linearly dispersing topological surface state which is protected from backscattering. Although magnetic susceptibility measurements undoubtedly confirm the Meissner effect, suggesting a superconducting volume fraction close to 100%, our highly surface sensitive STS data indicate that the surface of both materials is normal conducting. Precise analysis of LLS data obtained on $Tl_{0.6}Bi_2Te_3$ reveals that—compared to earlier ARPES data[25]—the surface is moderately n-shifted, placing the chemical potential right into the band gap where the density of states is minimal. Doping the surface with Cu adatoms resulted in a very significant downwards (n-type) surface band bending which—due to the rather low carrier density near the surface—will reach rather deep into the bulk. Potentially, this downward band bending leads to a further decoupling of the n-doped surface from the p-doped $Tl_{0.6}Bi_2Te_3$ bulk. One possibility to overcome the issue of a p–n junction which isolates the surface from the bulk might be through "hole" doping the $Tl_{0.6}Bi_2Te_3$ surface with a suitable atom/molecule, such as C_{60}.

Another result of our study is that even gentle collisions of the STM tip with any of the two materials investigated here, i.e., $Tl_{0.6}Bi_2Te_3$ or $Nb_xBi_2Se_3$, lead to superconducting tips. For

both materials, temperature- and field-dependent measurements reveal very similar values for the critical temperature and the critical field of $T_C \approx 5\,\text{K}$ and $\mu_0 H_{C_2} \approx 5\,\text{T}$, respectively. It appears that—even though both the surfaces of extended single crystals and the W tip are normal conducting themselves—the combinations of W plus the nanoparticles picked up by STM tip very reliably exhibit a superconducting gap which survives up to critical temperatures or external magnetic fields well above the corresponding bulk values. The large critical field could be due to a finite-size effect, but the enhancement in T_C cannot be explained in this way, thereby pointing to a new superconducting phase. In this regard, it is useful to mention that W has a tendency towards superconducting instability.[38] Future dedicated studies on nanoparticles will be necessary to test this hypothesis.

IV. CONCLUSION

In conclusion, we analyzed the surface structural and electronic properties of $Tl_{0.6}Bi_2Te_3$ and $Nb_xBi_2Se_3$ by low-temperature scanning tunneling spectroscopy. We could clearly demonstrate the existence of a topological surface state by Landau level spectroscopy and quasiparticle interference. The not-so-occasional observation of gapped tunneling spectra is ascribed to tips which were unintentionally coated with superconducting material. In these cases both the critical temperature and the critical magnetic field are about a factor of 3–10 higher than in bulk sensitive experiments. In agreement with this hypothesis we could not find any hint of magnetic vortices in field-dependent measurements. We conclude that the topological surface state of cleaved $Tl_{0.6}Bi_2Te_3$ and $Nb_xBi_2Se_3$ surfaces do not take part in the superconducting properties of these materials down to the lowest possible measurement temperatures of $300\,\text{mK}$.

---

* corresponding author: swilfert@physik.uni-wuerzburg.de

† Current address: 2D Crystal Consortium, Materials Research Institute, The Pennsylvania State University, University Park, Pennsylvania 16802, United States

[1] G. E. Volovik and V. M. Yakovenko, Journal of Physics: Condensed Matter **1**, 5263 (1989).

[2] G. E. Volovik, JETP Letters **55**, 363 (1992).

[3] M. Sato and Y. Ando, Reports on Progress in Physics **80**, 076501 (2017).

[4] C. Nayak, S. H. Simon, A. Stern, M. Freedman, and S. Das Sarma, Rev. Mod. Phys. **80**, 1083 (2008).

[5] N. Read and D. Green, Phys. Rev. B **61**, 10267 (2000).

[6] M. Stone and S.-B. Chung, Phys. Rev. B **73**, 014505 (2006).

[7] A. R. Akhmerov, J. Nilsson, and C. W. J. Beenakker, Phys. Rev. Lett. **102**, 216404 (2009).

[8] L. Fu and C. L. Kane, Phys. Rev. Lett. **100**, 096407 (2008).

[9] M.-X. Wang, C. Liu, J.-P. Xu, F. Yang, L. Miao, M.-Y. Yao, C. L. Gao, C. Shen, X. Ma, X. Chen, Z.-A. Xu, Y. Liu, S.-C. Zhang, D. Qian, J.-F. Jia, and Q.-K. Xue, Science **336**, 52 (2012).

[10] W. Dai, A. Richardella, R. Du, W. Zhao, X. Liu, C. X. Liu, S.-H. Huang, R. Sankar, F. Chou, N. Samarth, and Q. Li, Scientific Reports **7**, 7631 (2017).

[11] J.-P. Xu, M.-X. Wang, Z. L. Liu, J.-F. Ge, X. Yang, C. Liu, Z. A. Xu, D. Guan, C. L. Gao, D. Qian, Y. Liu, Q.-H. Wang, F.-C. Zhang, Q.-K. Xue, and J.-F. Jia, Phys. Rev. Lett. **114**, 017001 (2015).

[12] S. Nadj-Perge, I. K. Drozdov, B. A. Bernevig, and A. Yazdani, Phys. Rev. B **88**, 020407 (2013).

[13] S. Nadj-Perge, I. K. Drozdov, J. Li, H. Chen, S. Jeon, J. Seo, A. H. MacDonald, B. A. Bernevig, and A. Yazdani, Science **346**, 602 (2014).

[14] M. Ruby, F. Pientka, Y. Peng, F. von Oppen, B. W. Heinrich, and K. J. Franke, Phys. Rev. Lett. **115**, 197204 (2015).

[15] Y. S. Hor, A. J. Williams, J. G. Checkelsky, P. Roushan, J. Seo, Q. Xu, H. W. Zandbergen, A. Yazdani, N. P. Ong, and R. J. Cava, Phys. Rev. Lett. **104**, 057001 (2010).

[16] B. J. Lawson, Y. S. Hor, and L. Li, Phys. Rev. Lett. **109**, 226406 (2012).

[17] S. Sasaki, M. Kriener, K. Segawa, K. Yada, Y. Tanaka, M. Sato, and Y. Ando, Phys. Rev. Lett. **107**, 217001 (2011).

[18] N. Levy, T. Zhang, J. Ha, F. Sharifi, A. A. Talin, Y. Kuk, and J. A. Stroscio, Phys. Rev. Lett. **110**, 117001 (2013).

[19] K. Matano, M. Kriener, K. Segawa, Y. Ando, and G.-q. Zheng, Nature Physics **12**, 852 (2016).

[20] S. Yonezawa, K. Tajiri, S. Nakata, Y. Nagai, Z. Wang, K. Segawa, Y. Ando, and Y. Maeno, Nature Physics **13**, 123 (2017).

[21] Z. Liu, X. Yao, J. Shao, M. Zuo, L. Pi, S. Tan, C. Zhang, and Y. Zhang, Journal of the American Chemical Society **137**, 10512 (2015).

[22] Shruti, V. K. Maurya, P. Neha, P. Srivastava, and S. Patnaik, Phys. Rev. B **92**, 020506 (2015).

[23] G. Du, J. Shao, X. Yang, Z. Du, D. Fang, J. Wang, K. Ran, J. Wen, C. Zhang, H. Yang, Y. Zhang, and H.-H. Wen, Nature Communications **8**, 14466 (2017).

[24] Z. Wang, A. A. Taskin, T. Frölich, M. Braden, and Y. Ando, Chemistry of Materials **28**, 779 (2016).

[25] C. X. Trang, Z. Wang, D. Takane, K. Nakayama, S. Souma, T. Sato, T. Takahashi, A. A. Taskin, and Y. Ando, Phys. Rev. B **93**, 241103 (2016).

[26] Y. Qiu, N. Sanders, J. Dai, J. E. Medvedeva, W. Wu, P. Ghaemi, T. Vojta, and Y. S. Hor, arXiv **1512.03519** (2015).

[27] T. Asaba, B. J. Lawson, C. Tinsman, L. Chen, P. Corbae, G. Li, Y. Qiu, Y. S. Hor, L. Fu, and L. Li, Phys. Rev. X **7**, 011009 (2017).

[28] M. Kriener, K. Segawa, Z. Ren, S. Sasaki, S. Wada, S. Kuwabata, and Y. Ando, Phys. Rev. B **84**, 054513 (2011).

[29] Z. Wang, K. Segawa, S. Sasaki, A. A. Taskin, and Y. Ando, APL Materials **3**, 083302 (2015).

[30] T. Bathon, S. Achilli, P. Sessi, V. A. Golyashov, K. A. Kokh, O. E. Tereshchenko, and M. Bode, Advanced Materials **28**, 2183 (2016).

[31] Z. Alpichshev, J. G. Analytis, J.-H. Chu, I. R. Fisher, Y. L. Chen, Z. X. Shen, A. Fang, and A. Kapitulnik, Phys. Rev. Lett. **104**, 016401 (2010).

[32] Y. Okada, W. Zhou, C. Dhital, D. Walkup, Y. Ran, Z. Wang, S. D. Wilson, and V. Madhavan, Phys. Rev. Lett. **109**, 166407 (2012).

[33] P. Roushan, J. Seo, C. V. Parker, Y. S. Hor, D. Hsieh, D. Qian, A. Richardella, M. Z. Hasan, R. J. Cava, and A. Yazdani, Nature **460**, 1106 (2009).

[34] P. Sessi, M. M. Otrokov, T. Bathon, M. G. Vergniory, S. S. Tsirkin, K. A. Kokh, O. E. Tereshchenko, E. V. Chulkov, and M. Bode, Phys. Rev. B **88**, 161407 (2013).

[35] P. Sessi, F. Reis, T. Bathon, K. A. Kokh, O. E. Tereshchenko, and M. Bode, Nature Communications **5**, 5349 (2014).

[36] L. Fu, Phys. Rev. Lett. **103**, 266801 (2009).

[37] S. Wilfert, M. Schmitt, H. Schmidt, T. Mauerer, P. Sessi, H. Wang, Q. Mao, M. Fang, and M. Bode, Phys. Rev. B **97**, 014514 (2018).

[38] S. Basavaiah and S. R. Pollack, Journal of Applied Physics **39**, 5548 (1968).